Electronic structure of mixed-valence semiconductors in the LSDA+U approximation. I. Sm monochalcogenides

V. N. Antonov* and B. N. Harmon
Ames Laboratory, Iowa State University, Ames, Iowa 50011

A. N. Yaresko
Max Planck Institute CPFS, Nöthnitzer Str. 40, D-01187 Dresden, Germany

(Received 12 November 2001; revised manuscript received 14 March 2002; published 8 October 2002)

The electronic structure and optical spectra of Sm monochalcogenides are investigated theoretically from first principles, using the fully relativistic Dirac LMTO band structure method. The electronic structure is obtained with the local spin-density approximation (LSDA), as well as with the so-called LSDA+U approach. In contrast to LSDA, where the stable solution in SmS is a metal, the LSDA+U gave an insulating ground state. The energy band structure of samarium monochalcogenides describes well their measured x-ray photoemission spectra (XPS) as well as their optical spectra. The electronic structure of SmS high-pressure golden phase calculated in the LSDA+U approximation is characterized by five fully occupied $4f$ levels situated around 6 eV below the Fermi level and a sixth $4f$ level partly occupied due to pinning at the Fermi level. The occupation number is equal to 0.45 (valence 2.55+).

DOI: 10.1103/PhysRevB.66.165208 PACS number(s): 71.28.+d, 75.30.Mb

I. INTRODUCTION

Mixed valence (MV) phenomena occurring in rare earth compounds attracted a great deal of interest in the 1970s and early 1980s. (The history is well reviewed by Wachter.[1]) Such effects are expected to arise in systems where two electron configurations corresponding to $4f$ occupation numbers n and $n-1$ have nearly degenerate energies. So the ground state of a mixed valence compound is a quantum mechanical mixture of both the $4f^n$ and the $4f^{n-1}d$ configuration on each rare earth ion. Among MV compounds, there are a few cases where a narrow-gap behavior is known to exist at low temperature: SmS (high pressure golden phase), TmSe, SmB_6, YbB_{12}, UNiSn, $Ce_3Bi_4Pt_3$, etc. Although the burst of activity dealing with MV materials in the 1970s has been superseded by the subsequent shift of interest toward other strongly correlated electron systems (heavy fermions, high-temperature superconductors, etc.) some very fundamental questions were left unsettled. In recent years these questions are being revisited as a result of the insight gained in studying related systems, or simply because better samples or improved experimental techniques have become available.[2,3]

In the case of mixed valence semiconductors one of the most important questions is the microscopic mechanism for the band gap formation. Several mechanisms of gap formation in such systems have been proposed during the last two decades. Mott[4] and later Martin and Allen[5] argued that a narrow insulating gap, only a few meV wide, can occur in the electronic density of states (DOS) at the Fermi energy as a result of the strong *on-site* hybridization between the narrow $4f$ band and the broad conduction band. On the other hand, Kasuya and his group[6] introduced the concept of weak Wigner crystallization of the f electrons in the low carrier limit. Kikoin with co-workers calculated the electronic spectrum of SmS and SmB_6 using a model which considers MV semiconductors as excitonic insulators.[7] They describe the MV state in SmB_6 as a mixture of singlet states of divalent Sm(f^6) and the bound electron–hole pairs f^5b, where b is the state of an electron promoted from the f shell to p orbitals spread over neighboring boron sites but having the same symmetry as the f electron in a central site. We should also mention the anisotropic hybridization model with a pseudogap proposed by Hanzawa.[8] A gap structure containing intrinsic states was also found from studies of the extended Falicov-Kimball model.[9]

The electronic structure of SmS has attracted much attention during the last several decades because it shows an isostructural first-order phase transition under pressure.[1] The transition is accompanied by dramatic changes in the electronic system, manifesting itself in a spectacular color change from black to golden, and also in the lattice dynamics. For SmS under normal conditions (i.e., in the black phase), as well as for SmSe and SmTe, there is no doubt that these materials are semiconducting and that the samarium ions have valence 2+, or at most a very small deviation.[1] For the golden phase, the situation is not as clear. At pressures just above the phase transition, SmS is mixed valent, with a samarium valency of about 2.6 determined from spectroscopic methods and susceptibility measurements[10–12] and about 2.8 from the Vegards-law analysis of lattice constant measurements.[12] With further increasing pressure one gradually closes the hybridization gap in SmS and the temperature dependence of the resistivity turns to metallic behavior at low temperatures above 19.5 kbar with the valency increasing toward 3+.[13–15]

Standard band-structure calculations[16–19] in the local spin density approximation yield a spin–orbit splitting of about 0.6 eV between the $4f_{5/2}$ and the $4f_{7/2}$ states. At normal volume, these two sets of bands are crossed by the lowest $5d$ band resulting in a metallic behavior. The LSDA calculations provide an inadequate description of the $4f$ electrons in SmS due to improper treatment of correlation effects. In particular,

total energy versus volume LSDA calculations[19] underestimate the equilibrium lattice constant of SmS. Furthermore, these calculations showed that the bulk modulus agrees much better with the experimental value of the normal phase if the $4f$ states are treated as core states. Besides, LSDA calculations cannot account for the splitting of filled and empty f bands, which is expected to be 6–7 eV from x-ray photoemission spectroscopy[20] and bremsstrahlung isohromat spectra (BIS) measurements.[21] Attempts at a description beyond LSDA have been published, where the common idea is to distinguish occupied and unoccupied $4f$ states. One possibility is to approximate the self-energy by introducing the Coulomb repulsion U as an additional parameter to the one-particle (LSDA) equations for a quasiparticle band structure, as performed by Lópes-Aguilar and Costa-Quintana.[22] Consequently, they found a semiconducting state due to the Hubbard-type splitting between the occupied and unoccupied bands. Since the underlying uncorrelated band structure was calculated without taking into account relativistic effects, the results may have only qualitative significance. In a different approach, Schumann *et al.*[23] took into account the self-interaction correction (SIC) for the six relativistic states with total angular momentum $J=5/2$. Although the SIC-LSDA calculations produce the correct semiconductor ground state of SmS, the splitting between the occupied $4f_{5/2}$ and the unoccupied $4f_{7/2}$ states amounts to about 10 eV. This value is larger than the on-site Coulomb correlation energy estimated from XPS spectra $U\sim 6$ eV.[20] The SIC-LSDA calculations place the occupied $4f$ levels below S $3p$ states producing an energy gap between S $3p$ and Sm $5d$ states, however spectroscopic observations place the $4f_{5/2}$ states just below the Fermi energy and a gap occurs between Sm $4f_{5/2}$ and Sm $5d$ states.[1] Recently Lehner *et al.*[24] calculated the spectral density of SmS using a multiband periodic Anderson model. The s,p, and d states were treated as band states within the local spin-density approximation and the $4f$ shell treated as local many-electron states. The calculated spectral density was found to be in fair agreement with the measured photoemission and inverse photoemission spectra.

The aim of this work is to theoretically study the electronic structure and optical spectra of the mixed valence semiconductors SmX (X=S, Se, and Te), SmB_6, and YbB_{12}. The discussion above indicates there are still many questions concerning details of the electronic structure for the Sm compounds, and to the best of our knowledge their optical properties have not yet been calculated using first principles calculations. The results of such calculations can be compared to experimental spectra to provide information about occupied and unoccupied states near the Fermi level. We also report investigations of the electronic structure of $Sm_{0.5}La_{0.5}S$, $Sm_{0.5}Th_{0.5}S$, and LuB_{12} systems. We have divided the work into two parts, with this, paper I, concentrating on the electronic structure and optical properties of Sm monochalcogenides and related compounds, such as $Sm_{0.5}La_{0.5}S$ and $Sm_{0.5}Th_{0.5}S$. Paper II deals with SmB_6, YbB_{12} compounds and LuB_{12} as a reference material.

To better account for the on-site f-electron correlations, we have adopted as a suitable model the LSDA+U approach.[25] The LSDA+U method has proven to be an efficient and reliable tool for calculating the electronic structure of systems where the Coulomb interaction is strong (for a review, see Ref. 26). The LSDA+U approach was successfully applied to the heavy-fermion compounds YbPtBi (Ref. 27) and Yb_4X_3 (X=P, As, Sb, and Bi),[28] metal–insulator transition compound Fe_3O_4,[29] and mixed valence semiconductor UNiSn.[30] In our previous paper[31] we applied the LSDA+U method to the theoretical investigation of the electronic structure of mixed valent thulium monochalcogenides TmX (X=S, Se, and Te). The method describes well their measured BIS, x-ray, and ultraviolet photoemission spectra as well as the optical and magneto-optical spectra.

This paper is organized as follows: Sec. II presents a description of the crystal structure of the Sm monochalcogenides and the computational details. Section III is devoted to describing the electronic structure and optical properties of the Sm monochalcogenides at normal pressure as well as for the high pressure golden phase of SmS calculated in the LSDA and LSDA+U approximations. The theoretical optical calculations are compared to the experimental measurements. We also investigate theoretically the electronic structure of Th^{4+} and La^{3+} substituted SmS. Finally, the results are summarized in Sec. IV.

II. CRYSTAL STRUCTURE AND COMPUTATIONAL DETAILS

Sm monochalcogenides crystallize in the NaCl type crystal structure, and the space group is $Fm\bar{3}m$ (No. 225). In our band structure calculations we used the experimentally measured constants $a=5.972$, 6.202, and 6.595 Å for SmS, SmSe, and SmTe, respectively.[32]

The details of the computational method are described in our previous paper,[31] and here we only mention several aspects. The electronic structure of the compounds was calculated self-consistently using the local spin density approximation[33] and the fully relativistic spin-polarized LMTO method in the atomic-sphere approximation, including the combined correction (ASA+CC).[34–38] For the exchange and correlation potential the parametrization of von Barth and Hedin was used.[39] The combined correction terms have been included also in calculation of the optical matrix elements.[40] The Kramers-Kronig transformation has been used to calculate the dispersive parts of the optical conductivity from the absorptive parts. To improve the potential we include additional empty spheres in the 8c positions. The basis consisted of the Sm s, p, d, f, and g; S, Se, and Te s, p, and d, and empty sphere s, and p LMTO's. The **k**-space integrations were performed with the improved tetrahedron method[41] and charge self-consistently was obtained with 1305, 969, and 904 irreducible **k**-points in SmS, SmB_6, and YbB_{12}, respectively.

We have adopted the LSDA+U method[25] as a different level of approximation to treat electron–electron correlation. The Hubbard-type U_{eff} can be calculated from atomic Dirac-Hartree-Fock (DHF) (Ref. 42) or from Green-function impurity calculations,[43] and from band structure calculations in the super-cell approximation.[44] The calculated value of U_{eff} can depend on theoretical approximations and it may be bet-

ter to regard the value of U_{eff} as a parameter and try to specify it from comparison of the calculated physical properties with experiments. We estimated U_{eff} from the best agreement in relative position of the centroids of the Sm^{3+} and Sm^{2+} theoretically calculated and experimentally measured x-ray photoemission spectra. This yields $U_{\text{eff}} = 6.0$ eV in SmX (X= S, Se, and Te), 7.0 eV in SmB_6, and 8.0 eV in YbB_{12}. We found, however, that the optical spectra are rather insensitive to the precise value of U_{eff}. The LSDA+U band structure calculations with U_{eff} varying by ± 1 eV provide optical spectra in reasonable agreement with the experimental data. On the other hand, the value of the energy gap strongly depends on the value of U_{eff}. $U_{eff} = 6.0$ eV provides energy gaps in Sm monochalcogenides in a good agreement with the experimental data.

III. RESULTS AND DISCUSSION

A. Sm monochalcogenides

The Sm monochalcogenides offer the interesting possibility to study the transition from semiconductor to the MV state as a function of pressure. First, it is of great importance to characterize the semiconducting state.

In our band structure calculations we have performed three independent fully relativistic spin-polarized calculations. We consider the $4f$ electrons as (1) itinerant electrons using the local spin-density approximation; (2) fully localized, putting them in the core; and (3) partly localized using the LSDA+U approximation. We note that an important difference with respect to treating the $4f$ electrons as core electrons is that in the LSDA+U calculation all optical transitions from and to the $4f$ states are taken into account.

Figure 1 shows the energy band structure of SmS for all three approximations. The energy band structure of SmS with the $4f$ electrons in the core can be subdivided into three regions separated by energy gaps. The bands in the lowest region around -11 eV have mostly S s character with some amount of Sm sp character mixed in. The next six energy bands are S p bands separated from the s bands by an energy gap of about 7 eV. The width of the S p band is about 3.2 eV. The unoccupied electronic states can be characterized as Sm $5d$ bands. The sharp peaks in the DOS calculated in the LSDA just below and above the Fermi energy are due to $4f_{5/2}$ and $4f_{7/2}$ states, respectively (Fig. 1).

In our LSDA+U band structure calculations we started from a $4f^6$ configuration for the Sm^{2+} ion with six on-site $4f$ levels shifted downward by $U_{\text{eff}}/2$ and eight levels shifted upwards by this amount. The energies of occupied $4f_{5/2}$ and unoccupied $4f_{7/2}$ levels are separated by approximately U_{eff}. The LSDA+U energy bands and total density of states of SmS for $U_{\text{eff}}=6$ eV are shown in Fig. 1. The Coulomb repulsion U_{eff} strongly influences the electronic structure of SmS. For Sm^{2+} ions six $4f_{5/2}$ bands are fully occupied and situated in the gap between S p and Sm $5d$ states while the $4f_{7/2}$ hole levels are completely unoccupied and well above the Fermi level hybridized with Sm $5d$ states which results in a nonmagnetic ground state with the Sm ion in the divalent state. The theoretically calculated energy gap ΔE

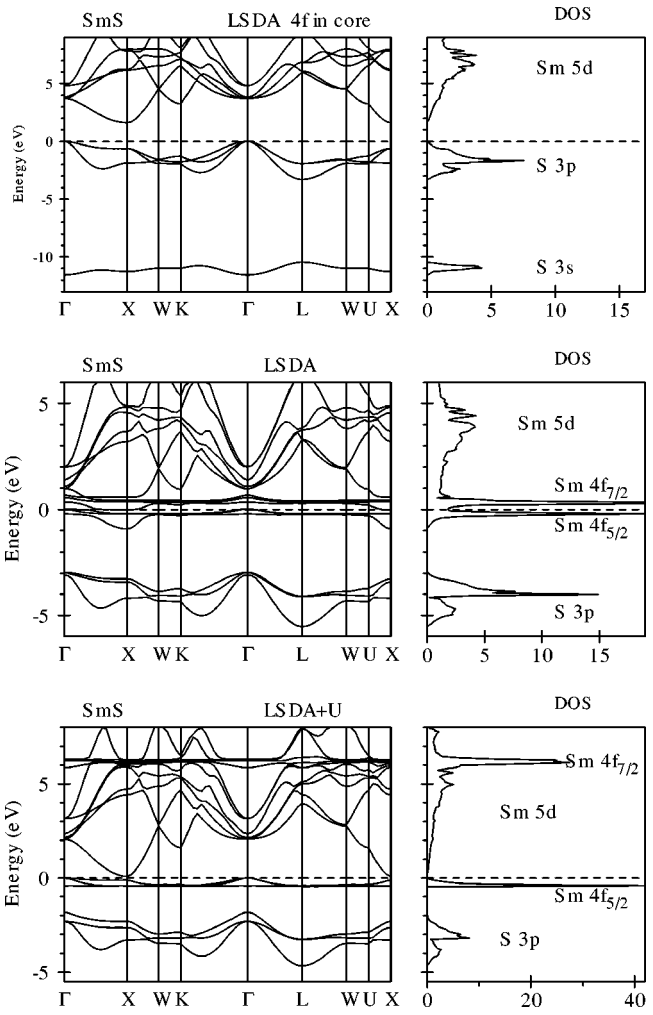

FIG. 1. Self-consistent fully relativistic, spin-polarized energy band structure and total DOS [in states/(unit cell eV))] calculated for SmS treating the $4f$ states as (1) fully localized ($4f$ in core); (2) itinerant (LSDA); and (3) partly localized (LSDA+U).

$=0.18$ eV which is formed between Sm $4f_{5/2}$ and Sm $5d$ states is in good agreement with the experimentally estimated 0.15 eV derived from the activation energy.[1]

The LSDA+U energy bands and total density of states of SmSe and SmTe for $U_{\text{eff}}=6$ eV are shown in Fig. 2. Their electronic structures are very similar to the SmS one with six Sm $4f_{5/2}$ bands fully occupied and the $4f_{7/2}$ hole bands completely unoccupied and well above the Fermi level hybridized with Sm $5d$ states. Theory gives energy gaps between Sm $4f_{5/2}$ and $5d$ bands equal to 0.47, and 0.67 eV in SmSe, and SmTe, respectively. The corresponding experimental values are equal to 0.45 and 0.65 eV.[1]

Photoemission experiments, both x-ray (XPS) and ultraviolet (UPS), have been of central importance for understanding mixed-valence materials (see the review of the early work by Campagna *et al.*[45]). In rare-earth photoemission, when the photon ejects an electron from the $4f^n$ shell it leaves behind a $4f^{n-1}$ configuration, hence the kinetic energy distribution curve of the emitted electron measures the spectra of the final-state hole. The final state $4f^{n-1}$ has a characteristic multiplet splitting which serves as a finger-

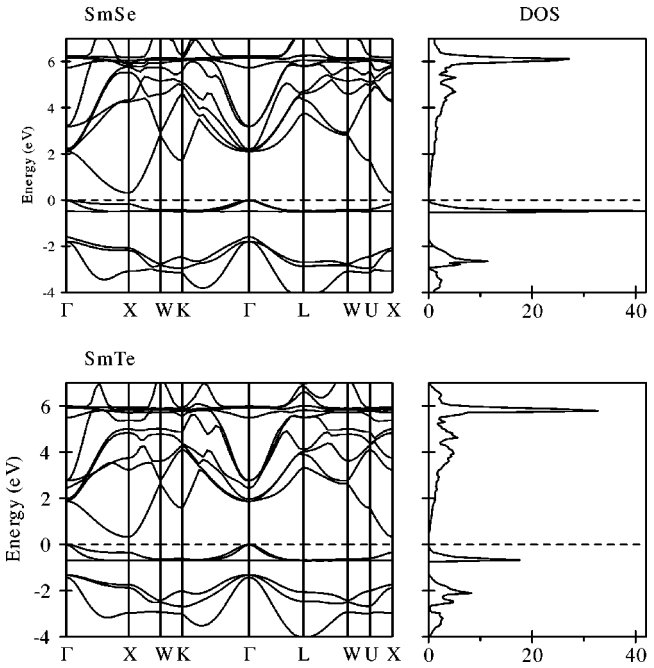

FIG. 2. Self-consistent fully relativistic, spin-polarized energy band structure and total DOS [in states/(unit cell eV)] calculated for SmSe and SmTe in the LSDA+U approximation.

print, and these are accurately resolved and calculable for rare-earth photoemission. By identification of the final-state hole the initial state can be inferred.

The partial $4f$ DOS of the occupied part of the SmS calculated in LSDA and LSDA+U approximations is compared with XPS measurements[20] in Fig. 3. The calculated $4f$ DOS has been broadened to account for lifetime effects and for experimental resolution. The Sm $4p$ states essentially do not contribute to the XPS spectra because of the low ionization cross section compared with that of the Sm $4f$ states.[46] Hence, the measurements only indicate the f excitation energies relative to the Fermi level. The theoretically calculated $4f$ DOS cannot, of course, fully account for the multiplet splitting. Therefore we present in Fig. 3 the $4f$ DOS's taking into account the multiplet structure of the $4f^5$ final state. We used the final state multiplet structure presented in Ref. 20. This multiplet structure consists of three terms ^{6}H, ^{6}F, and ^{6}P. The relative intensities for the multiplet peaks were obtained on the basis of Cox calculations[47] using the fractional parentage method.[48] In this method the Hund's rule ground state is assumed for n $4f$ electrons and then the coefficients of fractional parentage (Racah's) for the $n-1$ configurations are calculated. The intensities for the various configurations (multiplets) are just the square of the coefficients of fractional parentage. In Fig. 3 the XPS spectrum is modeled by a weighted sum of three $4f$ DOS curves. We aligned the centroid of the calculated occupied $4f$ DOS peak with the centroid of the atomic final state multiplet. Although, LSDA calculations produce almost the same picture as LSDA+U calculations in the case of SmS, for SmSe and SmTe the LSDA calculations place the $4f_{5/2}$ energy bands too close to the Fermi level which leads to disagreement with measured XPS spectra (Fig. 3).

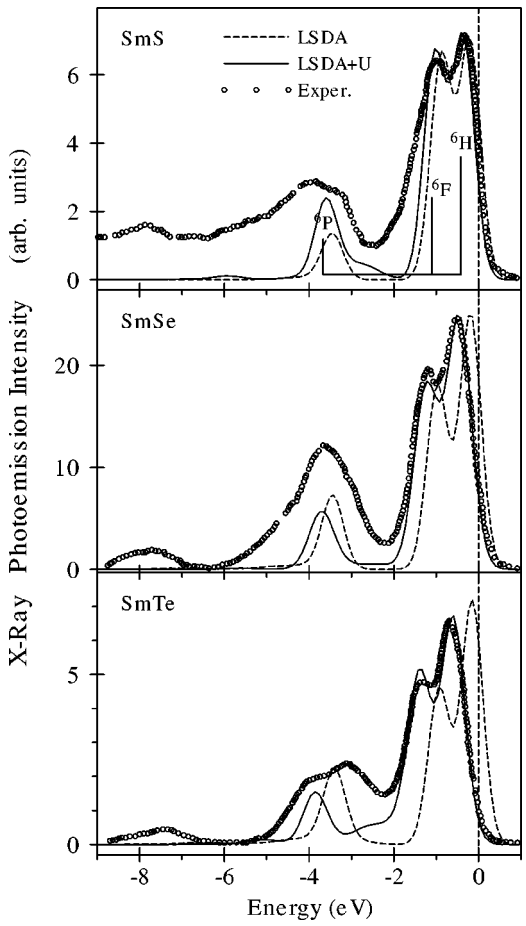

FIG. 3. Comparison of the calculated $4f$ DOS in the LSDA and LSDA+U approximations with the experimental XPS spectra from Ref. 20 taking into account the multiplet structure of the $4f^5$ final state (see explanations in the text).

From the good agreement between theory and XPS measurements we may conclude that the LSDA+U calculations give an accurate position for the occupied $4f$ bands. The principal question is the energy position of the empty $4f$ states, which is usually answered by optical or BIS measurements. Although optical measurements give more precise information on the band positions in comparison with XPS measurements due to much better resolution, they involve complex functions containing information of both the initial and final states simultaneously (joint density of states) and are strongly influenced by the optical transition matrix elements.

In Fig. 4 we show the experimental[49] real and imaginary parts of the dielectric function, $\varepsilon_{1xx}(\omega)$ and $\varepsilon_{2xx}(\omega)$, the optical reflectivity and optical conductivity $\sigma_{1xx}(\omega)$ spectra, as well as the spectra calculated with LSDA, LSDA+U and with the $4f$ electrons in the core. We mention, furthermore, that we have convoluted the calculated spectra with a Lorentzian whose width is 0.4 eV to approximate lifetime broadening. This picture clearly demonstrates that the better description is unambiguously given by the LSDA+U approach. As was mentioned above, the LSDA theory produces a metallic solution and, therefore, gives the wrong asymptotic behavior for the optical reflectivity and the dispersive part of the di-

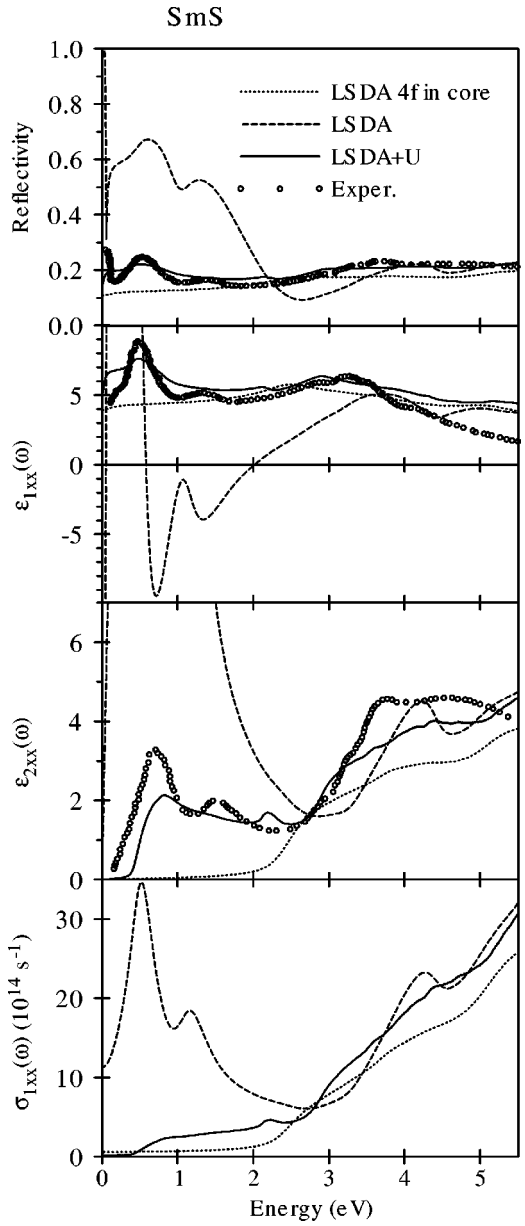

FIG. 4. Calculated optical reflectivity R, real and imaginary parts of the diagonal dielectric function, ε_{1xx}, ε_{2xx}, and diagonal part of the optical conductivity σ_{1xx} of SmS treating $4f$ states as (1) fully localized ($4f$ in core) (dotted line), (2) itinerant (dashed line), and (3) partly localized (LSDA+U approximation) (solid line) compared with experimental data (open circles) (Ref. 49).

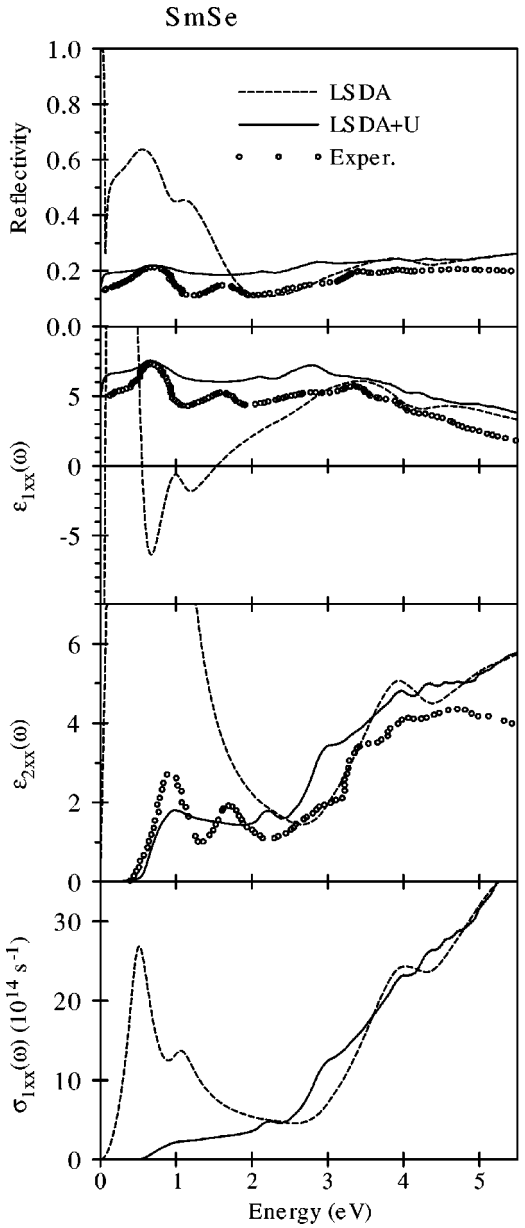

FIG. 5. Calculated optical reflectivity R, real and imaginary part of the diagonal dielectric function, ε_{1xx}, ε_{2xx}, and diagonal part of the optical conductivity σ_{1xx} of SmSe treating $4f$ states as (1) itinerant (dashed line) and (2) partly localized (LSDA+U approximation) (solid line) compared with experimental data (open circles) (Ref. 49).

electric function ε_{1xx} as $\omega \rightarrow 0$. The most prominent discrepancy in the LSDA spectra is the extra peaks between 0 and 1.5 eV in the $\varepsilon_{1xx}(\omega)$, $\varepsilon_{2xx}(\omega)$ and optical conductivity $\sigma_{1xx}(\omega)$ caused by interband transitions involving the occupied $4f_{5/2}$ and unoccupied $4f_{7/2}$ hybridized states. In the LSDA+U approach, the empty $4f_{7/2}$ state energies are shifted upward due to the on-site Coulomb interaction U_{eff}. As a result, the transitions involving the unoccupied $4f_{7/2}$ states do not take place at small photon energies, and the erroneous peak structures around 0–1.5 eV disappear from the optical spectra.

The calculations in which the $4f$ electrons are treated as quasicore are able to reproduce correct asymptotic behavior for the optical reflectivity and the dispersive part of the dielectric function ε_{1xx} as $\omega \rightarrow$ 0 similar to the LSDA+U calculations, but, it fails in producing a peak at around 0.6 eV in the absorptive part of the dielectric function ε_{2xx} and optical conductivity spectra. This peak is mostly determined by the $4f \rightarrow 5d$ interband transitions.

The LSDA+U theory also gives good agreement between calculated and measured optical spectra in the cases of SmSe (Fig. 5) and SmTe (not shown).

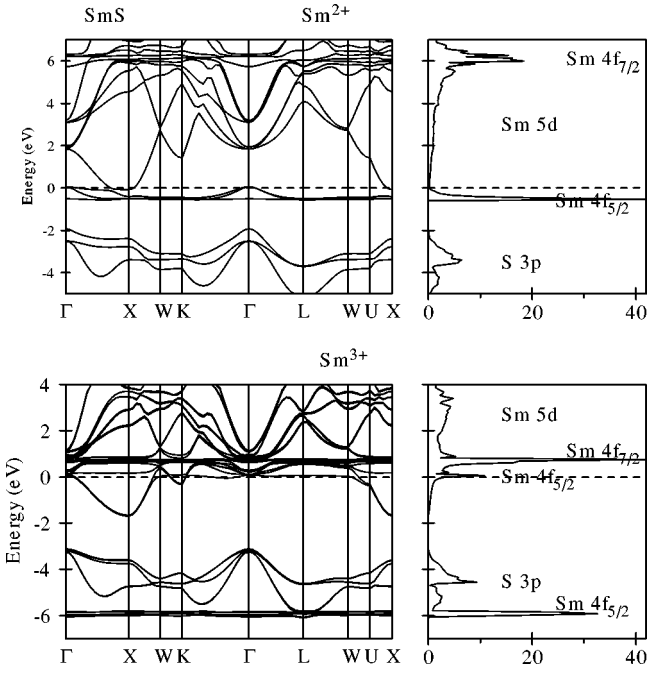

FIG. 6. Self-consistent fully relativistic, spin-polarized energy band structure and total DOS [in states/(unit cell eV)] calculated for SmS with the LSDA+U approximation for divalent and trivalent Sm atoms.

B. High pressure golden phase of SmS

The history of the Sm monochalcogenides as MV materials started at the beginning of the 1970s when Jayaraman *et al.*[50] and then Bucher *et al.*[51] discovered a pressure-induced semiconductor–metal transition and suggested that the metallic state would be mixed valent. It was a surprise that SmS showed this transition occurring at the incredibly low pressure of 6.5 kbar. Starting the pressure above the phase transition and decreasing, a large hysteresis is observed and the MV state snaps back to a semiconductor state at 1.5 kbar. For SmSe and SmTe the pressure-induced valence transition is continuous and is completed at higher pressures, about 45 and 60 kbar, respectively.[1]

By increasing external pressure and hence, decreasing the lattice constant, the widths of Sm $5d$ and $4f$ bands are increased. In addition, the crystal-field splitting of the $5d$ states e_g–t_{2g} in SmS is also increased. At a given pressure the $5d$ band overlaps with the $4f_{5/2}$ states and the energy gap becomes zero (Fig. 6). It happens at a lattice constant around 5.70 Å.[1] Starting from the overlap of $4f$ and $5d$ states, $4f$ electrons will spill into the $5d$ band leaving a $4f^5$ state behind. The ionic radius of Sm^{3+} is about 15% less than the radius of Sm^{2+}, so that simultaneously with more electrons in the $5d$ conduction band the lattice will shrink, thus further increasing the crystal-field splitting of the $5d$ states, resulting in an avalanche effect and a first-order valence transition. However, the valence transition does not go all the way to trivalency, but stops where the gain in electronic energy is compensated by an increase in lattice strain energy.[1]

The LSDA+U energy bands and total density of states of SmS for Sm^{3+} are shown in Fig. 6. There are five $4f_{5/2}$ bands fully occupied and hybridized with the bottom of the S p states. The $4f_{7/2}$ unoccupied states are well above the Fermi level. A 6th $4f_{5/2}$ hole level is partly occupied and pinned at the Fermi level. Although we used a starting configuration with zero occupation of the 6th $4f_{5/2}$ level, in the process of self-consistent relaxation the initially empty 6th $4f_{5/2}$ level becomes partly occupied due to pinning at the Fermi level with occupation number equal to 0.25 (valence 2.75+). It is a typical situation for mixed-valent crystals. We should mention here that partial occupation of the 6th $4f_{5/2}$ hole level in SmS is due to the hybridization effect between $5d$ and $4f$ energy band states.

We can use two different representations in the construction of the LSDA+U method, namely, (j,m_j) and (l,m_l) representations. Most of rare earths and their compounds have a rather large $4f$ spin magnetic moment, therefore it is natural to use the (l,m_l) representation in the calculations of their electronic structure.[27,28,31] In this case one chooses the projection of the orbital momentum onto the spin direction m_l for the occupied states. The SmS black phase as well as SmSe and SmTe have a nonmagnetic ground state, therefore we used in that case the (j,m_j) representation. For fully occupied $4f_{5/2}$ states the z projections of the total moment were equal to $m_j=-5/2,\ -3/2,\ -1/2,\ 1/2,\ 3/2$, and $5/2$.

The situation is not clear for golden SmS. We used both of the representations for the calculation of the electronic structure of the golden high pressure phase of SmS. Figure 6 presents the energy band structure of golden SmS in the (j,m_j) representation with $m_j=-1/2$ for the hole state. Due to the existence of a hole in the $4f_{5/2}$ shell the LSDA+U gives a so-called low magnetic moment ground state with total magnetic moment equal to 0.240 μ_B (spin and orbital moments have opposite directions with values equal to -0.305 and 0.545 μ_B, respectively). The (l,m_l) representation gives a high spin magnetic moment ground state in SmS with total magnetic moment equal to 4.636 μ_B at each Sm^{3+} site (spin and orbital moments have opposite directions with values equal to 5.501 and -0.865 μ_B, respectively). We should mention however, that although our LSDA+U band structure calculations give always a nonzero samarium magnetic moment, in golden SmS all the efforts to find a magnetic superstructure in high pressure SmS using neutron experiments have remained unsuccessful. However, one cannot exclude either a weak magnetic component below the limit of the experimental sensitivity (samples for high pressure measurements are very tiny) or an incommensurate structure giving peaks at positions not searched in the neutron experiments.[52] The evaluation of the magnetic ground state of golden SmS from first principles requires further investigation.[53–55]

The pinning of a partly occupied 6th $4f$ level strongly depends on the lattice constant. The increasing of the valency with decreasing of the lattice constant which was found in our band structure calculations can be considered as qualitative theoretical support of the conclusion derived from various experimental measurements,[1] that the application of pressure enhances the Sm^{3+} state relative to the Sm^{2+} state in SmS. The theoretically calculated samarium valency was found to be equal to 2.55+ and 2.86+ for high and low spin

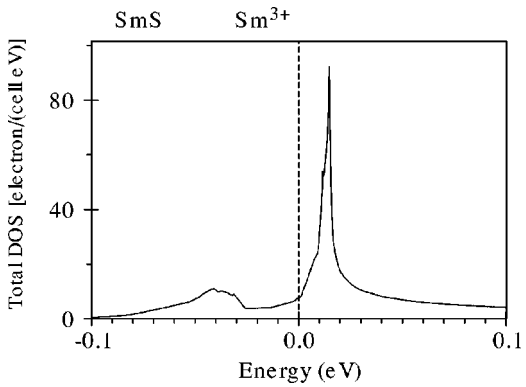

FIG. 7. Expanded view of the total DOS [in states/(unit cell eV)] of the high pressure golden phase of SmS in the LSDA+U approximation for low spin solution and $a=5.826$ Å.

solutions respectively. The experimentally estimated one is about 2.6+ from spectroscopic methods and susceptibility measurements[10–12] and about 2.8+ from the Vegards-low analysis of lattice constant measurements.[12]

Some experimental results indicate that the golden phase of SmS could be a narrow-gap semiconductor. Evidence for a gap comes from the activation behavior of the electrical resistivity and point contact measurements.[1] The estimations from the point-contact spectra shows a possible gap of about 6.4 meV.[1] On the other hand some experiments indicate that there may not be a gap but rather a pseudogap, and the hybridization does not occur over the whole Brillouin zone. Although the temperature dependence of the resistivity in the golden phase of SmS is semiconductor-like, the resistivity is increased only one order of magnitude with cooling from room temperature to several K's, whereas, e.g., in SmB_6 it is 5 orders of magnitude.[1] Direct optical measurements of mechanically polished (high pressure golden phase) SmS by Travaglini and Wachter[56] shows that, in contrast to SmB_6, the reflectivity does not tend to a constant value for $\omega \rightarrow 0$ but it seems to rise toward 100% as for a metal. Besides, there is a linear with T γ term in the specific heat presumably due to conduction electrons.[57] Our LSDA+U band structure calculations of golden SmS produce a pseudogap at the Fermi level with a peak just above and a shoulder below the Fermi level with predominantly of f character (Fig. 7). We should mention that when the density of states at E_F is small compared to the giant density of states of the f peaks, the resistivity may nevertheless appear activated over a certain temperature range as experimentally observed, but for the lowest temperatures metallic conductivity should persist.[56]

C. La^{3+} and Th^{4+} substituted SmS

It is well established that change in SmS, normally induced by pressure, can also be affected by the substitution of trivalent rare-earth ions, notably Y^{3+} or Gd^{3+} in the SmS lattice.[58] In this so-called *chemical collapse*, the SmS lattice undergoes an abrupt decrease in the lattice parameter at atmospheric pressure, when a certain critical concentration of the substitution is reached. This transition from semiconductor to MV metal is isostructural. Since all the above-mentioned substituting ions are much smaller in size relative to the Sm^{2+}, it appeared that the size of the ion was the principal factor involved in promoting the valence change, and that these smaller ions exert internal pressure on the lattice.[59] However, this chemical substitution not only creates lattice pressure but also introduces per trivalent ion one free carrier in the conduction band. There are also additional conduction electrons due to the valence transition, resulting from hybridization of f and d states. In the past, electronic and chemical pressure effects have not been separated and the chemical pressure effect alone was considered responsible for the valence transition.[60]

Later, Elmiger and Wachter[61] showed that SmSe doped with Ce in the absence of a lattice pressure (trivalent Ce ion has larger ionic radius than divalent Sm) nevertheless shows lattice softening and a tendency to become mixed valent. It was concluded that the valence transition is basically driven electronically and pressure is only an additional effect. Similar results were obtained in La doped SmS.[62] Trivalent La has almost the same ionic radius as divalent Sm. Nevertheless in spite of the missing lattice pressure the $Sm_{0.75}La_{0.25}S$ compound was found to be mixed valent at ambient pressure. Besides, the electrical resistivity as a function of temperature shows a clear-cut metallic behavior down to low temperatures and up to 1 kbar in this compound.[62] Finally Tsiok with co-workers[63] measured the volume change on SmSe and SmTe under the pressure, and, via conductivity, the energy gap. They clearly show that the energy gap was driven to zero before a softening of the lattice, therefore it is the concentration of carriers which triggers the lattice-related properties and not vice versa.[1]

In this work we calculated the electronic structure of La^{3+} and Th^{4+} doped SmS. The LSDA+U energy bands and total density of states of $Sm_{0.5}La_{0.5}S$ for Sm^{2+} and Sm^{3+} are shown in Fig. 8. The electronic structure of $Sm_{0.5}La_{0.5}S$ for trivalent Sm ions is similar to the high pressure golden SmS phase one (compare Figs. 6 and 8). In both cases five $4f_{5/2}$ bands are fully occupied and hybridized with the bottom of the S p states. The $4f_{7/2}$ unoccupied states are well above the Fermi level. A 6th $4f_{5/2}$ hole level is partly occupied and pinned at the Fermi level. The samarium occupation number in $Sm_{0.5}La_{0.5}S$ is equal to 0.15 (valence 2.85+). This is a typical situation for mixed-valent crystals. On the other hand, it is still not clear which mechanism is responsible for the $4f^6 \rightarrow 4f^5 5d$ transition. Looking at the band structure of $Sm_{0.5}La_{0.5}S$ with divalent samarium atoms (Fig. 8), we see that due to donation of an extra electron from trivalent La the Fermi level is shifted upward, while six $4f_{5/2}$ Sm bands are situated around 1 eV under the Fermi level hybridized with the bottom of the Sm $5d$ states.

Figure 9 shows the electronic structure of $Sm_{0.5}Th_{0.5}S$ for Sm^{2+} and Sm^{3+}. The main trend in the electronic structure of the sequence of Th and La doped SmS compounds results from the characteristic trend in the La $4f$ and Th $5f$ wave functions and from relativistic effects. Due to larger extension of the atomic $5f$ wave functions the empty Th $5f$ states are much wider in comparison to La $4f$ ones, and the former states are situated in the energy interval from around 2 to 5 eV above the Fermi level well hybridized with Sm $5d$ and

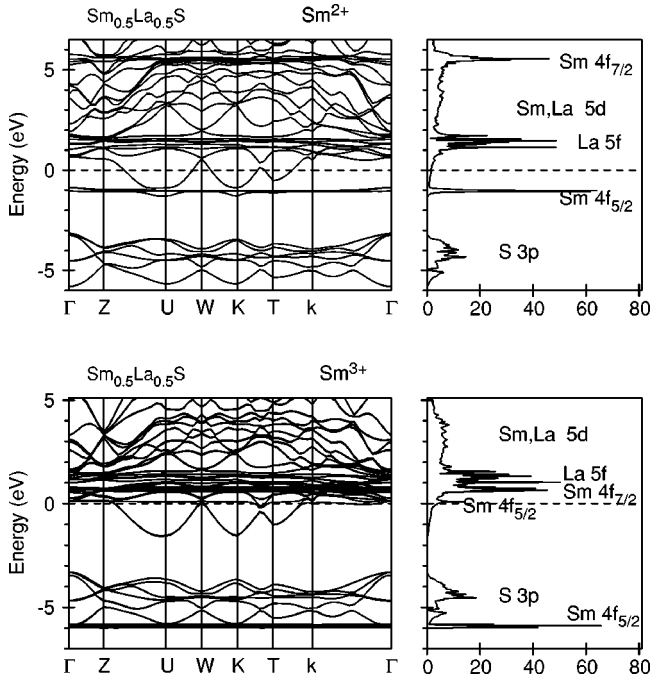

FIG. 8. Self-consistent fully relativistic, spin-polarized energy band structure and total DOS [in states/(unit cell eV)] calculated for $Sm_{0.5}La_{0.5}S$ in the LSDA+U approximation.

Th $6d$ states. Due to relativistic effects the Th $6d$ bandwidth is increased and its center of gravity is decreased in comparison to La $5d$ states. Besides, the Th ion has a valency of $4+$, therefore, it donates one extra electron to the valence band in comparison to La^{3+}. If one moves from La doped to Th doped SmS with divalent Sm atoms, six occupied $4f_{5/2}$ Sm bands move from the bottom of the d band upward about 1 eV (Fig. 9). The electronic structure of Th doped SmS with trivalent Sm atoms is also similar to La doped SmS with five $4f_{5/2}$ bands shifted down by the Coulomb repulsion U_{eff} at about 6 eV. The 6th $4f_{5/2}$ hole level is partly occupied and pinned at the Fermi level but with a much smaller occupation number of 0.03 (valence $2.97+$). So the LSDA+U band structure calculations produce an almost integer valent ground state for samarium ions in $Sm_{0.5}Th_{0.5}S$; divalent or almost trivalent ground states are obtained if we start our self-consistent procedure from Sm^{2+} or Sm^{3+}, respectively. On the other hand, XPS measurements clearly show that Th substituted SmS is a mixed valent system.[45]

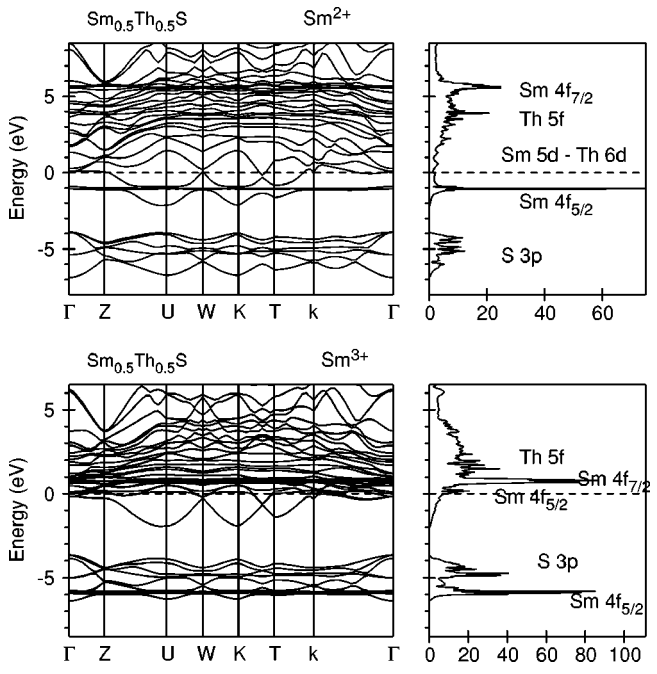

FIG. 9. Self-consistent fully relativistic, spin-polarized energy band structure and total DOS [in states/(unit cell eV)] calculated for $Sm_{0.5}Th_{0.5}S$ in the LSDA+U approximation for divalent and trivalent Sm atoms.

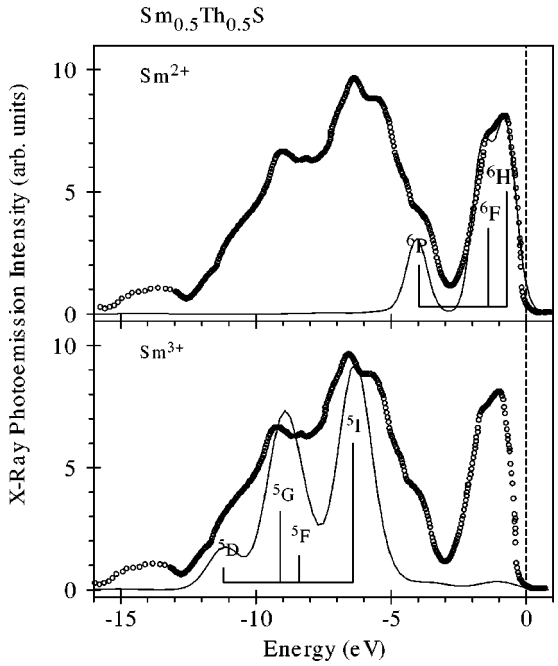

FIG. 10. Comparison the calculated $4f$ DOS in $Sm_{0.5}Th_{0.5}S$ using LSDA+U approximations with the experimental XPS spectra for $Sm_{0.85}Th_{0.15}S$ compound from Ref. 45 taking into account the multiplet structure of the $4f^4$ and $4f^5$ final states (see explanations in the text).

Figure 10 shows the XPS spectrum of the chemically collapsed MV $Sm_{0.85}Th_{0.15}S$ together with the theoretically calculated $4f$ DOS with the LSDA+U approximation taking into account the multiplet structure of the final states. The final state multiplet structure presented is from Ref. 45. As we mentioned above, the multiplet structure of Sm^{2+} ($4f^5$ finale state) has three terms ^6H, ^6F, and ^6P. Sm^{3+} for the $4f^4$ final state has the multiplets ^5I, ^5F, ^5G, and ^5D.[45] In Fig. 10 the XPS spectrum is modeled by a weighted sum of three LSDA+U $4f$ DOS curves for Sm^{2+} and four for the Sm^{2+} ion. We aligned the centroid of the calculated occupied $4f$ DOS peak with the centroid of the atomic final state multiplet. The agreement between theory and the UPS measurements is good. It is clear that the structures between 0.0 and -4.5 eV binding energy should be assigned to the final-state multiplet structure derived from six fully occupied $4f_{5/2}$

bands (Sm^{2+}) and the structures between -4.5 and -13 eV are associated with the final-state multiplet structure of the Sm^{3+} ions.

IV. SUMMARY

The Sm monochalcogenides SmS, SmSe, and SmTe constitute a very interesting system exhibiting behavior due to strongly correlated electrons. While the standard LSDA approach is unable to correctly describe the electronic structure of these materials because of the strong on-site Coulomb repulsion, U_{eff} the LSDA+U approach is remarkably accurate in providing detailed agreement with experiment for a number of properties. In this section we summarize these properties and the results of our work.

In contrast to LSDA, where the stable solution for Sm monochalcogenides at ambient pressure is metallic, the LSDA+U method gave an insulator with energy gaps of 0.15, 0.45, and 0.65 eV (the experimental gaps are 0.18, 0.47, and 0.67 eV) for SmS, SmSe, and SmTe, respectively. The Coulomb repulsion U_{eff} strongly influences the electronic structure of Sm monochalcogenides. For Sm^{2+} ions six $4f_{5/2}$ bands are fully occupied and situated in the gap between chalcogen $3p$ and Sm $5d$ states. The $4f_{7/2}$ hole levels are completely unoccupied and well above the Fermi level hybridized with Sm $5d$ states. LSDA+U theory predicts that the samarium ion in these compounds is in an integer divalent state. It also shows a gradual decreasing of the energy gap with reduction of the lattice constant. The LSDA+U theoretical calculations describe well the optical spectra of Sm monochalcogenides.

When applying external pressure to SmS and hence, decreasing its lattice constant the widths of Sm $5d$ and $4f$ bands are increased and the crystal-field splitting of the $5d$ states e_g–t_{2g} is also increased. At a given pressure the $5d$ band overlaps with the $4f_{5/2}$ states. This leads to a first-order valence $Sm^{2+} \rightarrow Sm^{3+}$ phase transition. The gap in SmS is closed at $a = 5.70$ Å in good agreement with experimental measurements of SmS transport properties under pressure. For SmS with Sm^{3+} ions five $4f$ bands are fully occupied and hybridize with chalcogenide p states. The initially empty hole 6th $4f$ level in the process of self-consistent relaxation becomes partly occupied with the $4f$ DOS maximum situated in close vicinity of the Fermi level in the golden phase of SmS. The occupation number of the 6th $4f$ hole level is equal to 0.45 (valence 2.55+) in a good agreement with the experimental estimates from spectroscopic methods and susceptibility measurements.

In conclusion, we would like to point out that while the LSDA+U approach does a very good job in the treatment of correlation effects in SmS, SmSe, and SmTe at normal pressure, it is still unclear how well it performs in describing the mixed valence state in golden SmS in the pressure range from 6 to 20 kbar. On one hand, we found the pinning of a partly occupied 6th $4f$ level at the Fermi level, which is the typical situation for mixed valence systems. On the other hand, LSDA+U calculations always produce a nonzero magnetic moment in the high pressure phase of SmS, although all attempts to find any sign of magnetic ordering in this system gave no positive results for the last 30 years. It is more likely that our LSDA+U calculations describe well the situation in the metallic phase of SmS at pressure $P \geqslant 20$ kbar with trivalent samarium ions (see Fig. 7).

We should mention that the experimental situation in golden SmS differs from that in SmB_6 in the sense that in the later system a new generation of samples of much better quality became available during recent years, and more reliable data about transport properties and infrared spectroscopy were obtained. In SmS we still use old experimental data and it is difficult to ascertain the full validity of measured gaps or pseudogaps as well as other properties based on the experiments of the early 1970s. The physical nature of the mixed valence state in golden SmS requires further investigation theoretically as well as experimentally.

ACKNOWLEDGMENTS

This work was carried out at the Ames Laboratory, which is operated for the U.S.Department of Energy by Iowa State University under Contract No. W-7405-82. This work was supported by the Director for Energy Research, Office of Basic Energy Sciences of the U.S. Department of Energy. V.N. Antonov gratefully acknowledges the hospitality at Ames Laboratory during his stay. The authors are very grateful to Professor T. Suzuki for the suggestion to calculate the electronic structure of samarium monochalcogenides and for useful discussions. The authors are very grateful to Professor K. Kikoin for reading the manuscript and for fruitful discussions.

*Permanent address: Institute of Metal Physics, 36 Vernadskii Street, 252142 Kiev, Ukraine.

[1] P. Wachter, *Handbook of the Physics and Chemistry of Rare Earths*, edited by K. A. Gschneidner, L. Eyring, and S. Hüfner (North–Holland, Amsterdam, 1994), Vol. 19, p. 177.
[2] P. S. Riseborough, Adv. Phys. **49**, 257 (2000).
[3] L. Degiorgi, Rev. Mod. Phys. **71**, 687 (1999).
[4] N. F. Mott, Philos. Mag. **30**, 403 (1973).
[5] R. M. Martin and J. M. Allen, J. Appl. Phys. **50**, 7561 (1979).
[6] T. Kasuya, J. Phys. Colloq. **37**, C4 (1976); T. Kasuya, K. Takegahara, and T. Fujita, *ibid.* **40**, C5 (1979); **40**, 308 (1979); T. Kasuya, Europhys. Lett. **26**, 277 (1994).
[7] K. A. Kikoin, Zh. Éksp. Teor. Fiz. **85**, 1000 (1983) [JETP **58**, 582 (1983)]; J. Phys. C **17**, 6771 (1984); K. A. Kikoin and A. S. Mishenko, J. Phys. C **2**, 6491 (1990); S. Curnoe and K. A. Kikoin, Phys. Rev. B **61**, 15 714 (2000).
[8] K. Hanzawa, J. Magn. Magn. Mater. **177-181**, 347 (1998).
[9] M. Park and J. Hong, J. Korean Phys. Soc. **33**, 480 (1998).
[10] A. F. Sovestnov, V. A. Shaburov, L. A. Markova, and E. M. Savitski, Fiz. Tverd. Tela (Leningrad) **23**, 2827 (1981) [Sov. Phys. Solid State **23**, 1652 (1981)].
[11] J. M. D. Coey, S. K. Glatak, M. Avignon, and P. Holtzberg, Phys. Rev. B **14**, 3744 (1976).
[12] M. B. Maple and D. Wohleben, Phys. Rev. Lett. **14**, 3744 (1976).
[13] F. Holzberg and J. Wittig, Solid State Commun. **40**, 315 (1981).
[14] F. Lapierre, M. Ribault, F. Holzberg, and J. Floquet Solid State

Commun. **40**, 347 (1981).
[15] M. Konczukowski, J. Morillo, and H. P. Senateur, Solid State Commun. **40**, 517 (1981).
[16] H. L. Davis, in *Proceedings of the 9th Rare Earth Conference, Blacksburg, 1971* (Elsevier, Amsterdam, 1977).
[17] O. V. Farberovich, Fiz. Tverd. Tela (Leningrad) **22**, 669 (1980) [Sov. Phys. Solid State **22**, 393 (1980)]; Phys. Status Solidi B **104**, 365 (1981)].
[18] P. Strange, J. Phys. C **17**, 4273 (1984); Physica B & C **130**, 44 (1985).
[19] Z. W. Lu, D. J. Singh, and H. Krakauer, Phys. Rev. B **37**, 10 045 (1988).
[20] M. Campagna, E. Bucher, G. K. Wertheim, and L. D. Longinotti, Phys. Rev. Lett. **33**, 165 (1974).
[21] S.-J. Oh and J. W. Allen, Phys. Rev. B **29**, 589 (1984).
[22] F. López-Aguilar and H. Krakauer, J. Phys. C **19**, 2485 (1986); F. López-Aguilar, *ibid.* **19**, L735 (1986); S. Balle, J. Costa-Quintana, and F. Lṕez-Aguilar, Phys. Rev. B **37**, 6615 (1988).
[23] R. Schumann, M. Richter, L. Steinbeck, and H. Eschrig, Phys. Rev. B **52**, 8801 (1995).
[24] C. Lehner, M. Richter, and H. Eschrig, Phys. Rev. B **58**, 6807 (1998).
[25] V. I. Anisimov, J. Zaanen, and O. K. Andersen, Phys. Rev. B **44**, 943 (1991).
[26] V. I. Anisimov, F. Aryasetiawan, and A. I. Lichtenstein, J. Phys.: Condens. Matter **9**, 767 (1997).
[27] P. M. Oppeneer, V. N. Antonov, A. N. Yaresko, A. Ya. Perlov, and H. Eschrig, Phys. Rev. Lett. **78**, 4079 (1997).
[28] V. N. Antonov, A. N. Yaresko, A. Ya. Perlov, P. Thalmeier, P. Fulde, P. M. Oppeneer, and H. Eschrig, Phys. Rev. B **58**, 5043 (1998).
[29] V. N. Antonov, B. N. Harmon, V. P. Antropov, A. Ya. Perlov, and A. N. Yaresko, Phys. Rev. B **64**, 134410 (2001).
[30] P. M. Oppeneer, A. N. Yaresko, A. Ya. Perlov, V. N. Antonov, and H. Eschrig, Phys. Rev. B **54**, R3706 (1996).
[31] V. N. Antonov, B. N. Harmon, and A. N. Yaresko, Phys. Rev. B **63**, 205112 (2001).
[32] P. Villars and L. D. Calvert, *Pearson's Handbook of Crystallographic Data for Intermetallic Phases* (ASM International, Materials Park, 1991).
[33] U. von Barth and L. A. Hedin, J. Phys. C **5**, 1692 (1972).
[34] V. V. Nemoshkalenko and V. N. Antonov, *Computational Methods in Solid State Physics* (Gordon and Breach, London, 1998).
[35] O. K. Andersen, Phys. Rev. B **12**, 3060 (1975); D. D. Koelling and B. N. Harmon, J. Phys. C **10**, 3107 (1977).
[36] V. V. Nemoshkalenko, A. E. Krasovskii, V. N. Antonov, Vl. N. Antonov, U. Fleck, H. Wonn, and P. Ziesche, Phys. Status Solidi B **120**, 283 (1983).
[37] V. N. Antonov, A. Ya. Perlov, A. P. Shpak, and A. N. Yaresko, J. Magn. Magn. Mater. **146**, 205 (1995).
[38] H. Ebert, Phys. Rev. B **38**, 9390 (1988).
[39] L. Hedin and B. I. Lindqvist, J. Phys. C **4**, 2064 (1971).
[40] V. N. Antonov, A. I. Bagljuk, A. Ya. Perlov, V. V. Nemoshkalenko, Vl. N. Antonov, O. K. Andersen, and O. Jepsen, Low Temp. Phys. **19**, 494 (1993).
[41] P. E. Blöchl, O. Jepsen, and O. K. Andersen, Phys. Rev. B **49**, 16223 (1994).
[42] J. F. Herbst and J. W. Wilkins, in *Handbook of the Physics and Chemistry of Rare Earths*, edited by K. A. Gschneidner, L. Eyring, and S. Hüfner (North–Holland, Amsterdam, 1987), Vol. 10, p. 321.
[43] P. H. Dederics, S. Blügel, R. Zeller, and H. Akai, Phys. Rev. Lett. **53**, 2512 (1984).
[44] V. I. Anisimov and O. Gunnarsson, Phys. Rev. B **43**, 7570 (1991).
[45] M. Campagna, G. K. Wertheim, and E. Bucher, *Structure and Bonding* (Springer, Berlin, 1976), Vol. 30, p. 99.
[46] J. J. Yeh and I. Lindau, At. Data Nucl. Data Tables **32**, 1 (1985).
[47] P. A. Cox, *Structure and Bonding* (Springer, Berlin, 1975), Vol. 24, p. 59.
[48] G. Racah, Phys. Rev. **76**, 1352 (1949).
[49] B. Batlogg, E. Kaldis, A. Schlegel, and P. Wachter, Phys. Rev. B **14**, 5503 (1976).
[50] A. V. Jayaraman, V. Narayanamurti, E. Bucher, and R. G. Maines, Phys. Rev. Lett. **25**, 368 (1970); **25**, 1430 (1970).
[51] E. Bucher, V. Narayanamurti, and A. V. Jayaraman, J. Appl. Phys. **42**, 1741 (1971).
[52] J.-M. Mignot (private communication).
[53] P. Fulde, *Electron Correlations in Molecules and Solids* (Springer, Berlin, 1995).
[54] T. M. Rice and K. Ueda, Phys. Rev. B **34**, 6420 (1986).
[55] J. Lagsgaard and A. Svane, Phys. Rev. B **58**, 12 817 (1998).
[56] G. Travaglini and P. Wachter, Phys. Rev. B **30**, 5877 (1984).
[57] S. D. Bader, N. E. Phillips, and D. B. McWhan, Phys. Rev. B **7**, 4686 (1973).
[58] A. Jayaraman and R. G. Maines, Phys. Rev. B **19**, 4154 (1979).
[59] A. Jayaraman, P. D. Dernler, and L. D. Longinott, in *Valence Instabilites and Related Narrow Band Phenomena*, edited by R. D. Parks (Plenum, New York, 1977), p. 61.
[60] A. Jayaraman, in *Handbook of the Physics and Chemistry of Rare Earths*, edited by K. A. Gschneidner, L. Eyring, and S. Hüfner (North–Holland, Amsterdam, 1979), Vol. 2, p. 575.
[61] M. W. Elmiger and P. Wachter, J. Magn. Magn. Mater. **63&64**, 612 (1987).
[62] P. Wachter, A. Jung, and P. Steiner, Phys. Rev. B **51**, 5542 (1995).
[63] O. B. Tsiok, V. A. Sidorov, V. V. Bredikhin, L. G. Khvostantsev, A. V. Golubkov, and L. A. Smirnov, Solid State Commun. **79**, 227 (1991).